JVI Journals.ASM.org

Characterization of a Broadly Neutralizing Monoclonal Antibody That Targets the Fusion Domain of Group 2 Influenza A Virus Hemagglutinin

Gene S. Tan,[a] Peter S. Lee,[c,d] Ryan M. B. Hoffman,[c] Beryl Mazel-Sanchez,[a] Florian Krammer,[a] Paul E. Leon,[a] Andrew B. Ward,[c] Ian A. Wilson,[c,d] Peter Palese[a,b]

Department of Microbiology[a] and Department of Medicine,[b] Icahn School of Medicine at Mount Sinai, New York City, New York, USA; Department of Integrative Structural and Computational Biology[c] and The Skaggs Institute for Chemical Biology,[d] The Scripps Research Institute, La Jolla, California, USA

ABSTRACT

Due to continuous changes to its antigenic regions, influenza viruses can evade immune detection and cause a significant amount of morbidity and mortality around the world. Influenza vaccinations can protect against disease but must be annually reformulated to match the current circulating strains. In the development of a broad-spectrum influenza vaccine, the elucidation of conserved epitopes is paramount. To this end, we designed an immunization strategy in mice to boost the humoral response against conserved regions of the hemagglutinin (HA) glycoprotein. Of note, generation and identification of broadly neutralizing antibodies that target group 2 HAs are rare and thus far have yielded only a few monoclonal antibodies (MAbs). Here, we demonstrate that mouse MAb 9H10 has broad and potent *in vitro* neutralizing activity against H3 and H10 group 2 influenza A subtypes. In the mouse model, MAb 9H10 protects mice against two divergent mouse-adapted H3N2 strains, in both pre- and postexposure administration regimens. *In vitro* and cell-free assays suggest that MAb 9H10 inhibits viral replication by blocking HA-dependent fusion of the viral and endosomal membranes early in the replication cycle and by disrupting viral particle egress in the late stage of infection. Interestingly, electron microscopy reconstructions of MAb 9H10 bound to the HA reveal that it binds a similar binding footprint to MAbs CR8020 and CR8043.

IMPORTANCE

The influenza hemagglutinin is the major antigenic target of the humoral immune response. However, due to continuous antigenic changes that occur on the surface of this glycoprotein, influenza viruses can escape the immune system and cause significant disease to the host. Toward the development of broad-spectrum therapeutics and vaccines against influenza virus, elucidation of conserved regions of influenza viruses is crucial. Thus, defining these types of epitopes through the generation and characterization of broadly neutralizing monoclonal antibodies (MAbs) can greatly assist others in highlighting conserved regions of hemagglutinin. Here, we demonstrate that MAb 9H10 that targets the hemagglutinin stalk has broadly neutralizing activity against group 2 influenza A viruses *in vitro* and *in vivo*.

Influenza is a highly infectious respiratory disease that remains a public health problem worldwide. Seasonal influenza epidemics cause on average 3 to 5 million cases of severe illness and up to 250,000 to 500,000 deaths annually (1). In addition, sporadic zoonotic transmissions from avian or swine species are always a cause for concern.

Vaccination affords the best preexposure protection against influenza virus infection, although the vaccine must be annually reformulated to match the predicted circulating strains (2, 3). In the case of postexposure therapy, M2 ion channel blockers (e.g., amantadine and rimantadine) and neuraminidase inhibitors (i.e., oseltamivir and zanamivir) can be used as antiviral therapies. However, the emergence of resistant influenza A viruses quickly obviates the value of antiviral drugs, as in the case of the adamantane class of molecules (4). Thus, there is a need to develop better vaccines and antiviral compounds to combat influenza virus infections, while accommodating antigenic drifts and/or shifts.

The antibody response against hemagglutinin (HA), the major surface glycoprotein on influenza viruses, is an indispensable component in the overall immune response to influenza A virus. In fact, antibodies generated against the HA are the major metric by which immunity to influenza is measured and they fall into two basic categories: globular- and stalk-directed antibodies. Antibodies that possess hemagglutination-inhibiting (HAI) activity elicited against the globular domain during natural infection or vaccination is widely accepted as a correlate of protection against influenza (5, 6). However, due to the high mutability (antigenic drift) of the globular head region, HAI-active antibodies typically neutralize only closely related strains, although recent reports have shown that the HA receptor binding site can be more broadly recognized (7–13). In contrast, a smaller proportion of the antibodies elicited is directed against the membrane proximal stalk region of the HA. Due to its role in facilitating the fusion of the viral and endosomal membranes, which subsequently releases the viral ribonucleoprotein (RNP) into the cytosol, the stalk is less susceptible to mutations and is relatively conserved across the

Received 7 August 2014 **Accepted** 5 September 2014
Published ahead of print 10 September 2014
Editor: T. S. Dermody
Address correspondence to Peter Palese, peter.palese@mssm.edu.

doi:10.1128/JVI.02289-14

divergent subtypes. Thus, stalk-directed antibodies are capable of neutralizing diverse influenza viruses (14–27).

There are currently 18 known influenza A subtypes that can be divided into two major phylogenetic groups. The majority of the stalk-directed broadly neutralizing monoclonal antibodies (MAbs) that have been isolated and characterized to date bind and neutralize group 1 influenza A viruses (i.e., H1, H2, and H5 subtypes) (14–21), while only a few MAbs recognize group 2 influenza A viruses (e.g., H3, H7, and H10 subtypes) (22–24). Of note, human MAb FI6v3 was described to bind group 1 and 2 influenza A viruses (25), whereas human MAb CR9114 was found to bind to influenza A and B viruses (26). The mouse MAb 12D1 was the first antibody described to have pan-H3 binding and neutralizing activity and its epitope has been mapped to the N terminus of the long α-helix of the stalk domain (24). Others, such as CR8020 and CR8043, have been subsequently isolated from humans with broader binding and neutralizing profiles, revealing conserved epitopes at the base of the HA stalk common to group 2 HAs (22, 23). The discovery that broadly neutralizing antibodies against the HA can be isolated from both humans and mice reveal the presence of highly conserved epitopes in the stalk region of HA. Such broadly neutralizing antibodies have potential therapeutic value in high-risk groups, which include infants, the elderly, and immunocompromised patients. Moreover, analyses of these conserved epitopes may ultimately assist in the development of broad-spectrum influenza virus vaccines.

Thus, in order to identify other conserved epitopes in the H3 HA stalk, we utilized a similar strategy to boost the antibody response toward the HA stalk region (24, 27). A mouse was sequentially immunized with sublethal doses of three divergent H3N2 influenza A viruses and screened for reactivity against divergent H3 HAs. Here, we report the discovery of mouse MAb 9H10, which has broad neutralizing activity against group 2 influenza viruses.

MATERIALS AND METHODS

Cells, viruses, and purified viral proteins. Madin-Darby canine kidney (MDCK) and human embryonic kidney (HEK) 293T cells were maintained in Dulbecco Modification of Eagle Medium (DMEM; Mediatech, Inc.) supplemented with 10% fetal bovine serum (Invitrogen, Inc.) and penicillin (100 U/ml)–streptomycin (100 μg/ml). The following viruses were grown in 10-day-old specific-pathogen-free (SPF) embryonated chicken eggs (Charles River Laboratories, Inc.): A/Hong Kong/1/1968 (HK/68) (H3N2), A/Scotland/840/1974 (Scot/74) (H3N2), A/Alabama/1981 (AL/81) (H3N2), A/Panama/2007/1999 (Pan/99) (H3N2), A/Beijing/47/1992 (BJ/92) (H3N2), A/Wyoming/1/2005 (WY/05) (H3N2), A/Brisbane/10/2007 (Bris/07) (H3N2), A/Perth/16/2009 (Perth/09) (H3N2), A/Victoria/361/2011 (Vic/11) (H3N2), A/mallard/Interior Alaska/10BM 01929/2010 (AK/10) (H10N7), A/rhea/North Carolina/1993 (NC/93) (H7N1), and A/Czechoslovakia/1956 (CZ/56) (H4N6). The following reassortant viruses that have six internal proteins of A/Puerto Rico/8/34 (PR/8) (H1N1) expressing the HA and neuraminidase (NA) of the indicated viruses were also grown in 10-day-old SPF embryonated chicken eggs: cH5/3 (HA head domain of A/Vietnam/1203/04 [VN/04, H5] and the stalk region of Perth/09), cH7/3 (HA head domain of A/Shanghai/1/13 [SH/13, H9] and the stalk region of Perth/09), X-31 (HA and NA of HK/68) (rHK/68), X-79 (HA and NA of A/Philippines/2/82, H3N2) (rPhil/82), rVN/04 (HA lacking the polybasic cleavage site and NA of VN/04, H5N1), and rSH/13 (HA and NA of SH/13, H7N9). The reassortant virus A/California/4/2009 (rCA/09) (H1N1) with the internal genes of PR/8 was grown in MDCK cells.

The following purified baculovirus-expressed HA proteins were obtained from BEI Resources: Bris/07 (NR-19238), Perth/09 (NR-19442), A/New York/55/2004 (NR-19241), A/Wisconsin/67/2005 (NR-15171), A/Uruguay/716/2007 (NR-15168), and CA/09 (NR-15749). The following purified baculovirus-expressed HA proteins were synthesized in-house as described before (28, 29): Phil/82, Pan/99, CZ/56, A/mallard/Alberta/2007 (H7), AK/10, A/mallard/Gurjev/263/1982 (H14), A/shearwater/West Australia/2576/1979 (H15), A/mallard/Interior/7MP0167/2007 (H12), and A/black headed gull/Sweden/1/1999 (H13).

Generation of MAbs, screening, and purification. The generation of MAbs was previously reported (24, 27) with some modifications described below. A 6- to 8-week-old female BALB/c mouse (Jackson Laboratories, Inc.) was sequentially infected intranasally with 100,000 PFU of rPhil/82, Vic/11, and HK/68 viruses in 3-week intervals, followed by an intraperitoneal boost of a purified preparation (100 μg) of Perth/09 virus supplemented with 5 μg of R848 (Invivogen, Inc.) 3 weeks after the last immunization. Three days after the boost, the mouse was sacrificed, the spleen harvested and dissociated with a 10-ml 20-gauge needle into a single cell suspension in serum-free 1× DMEM. Splenocytes and SP2/0 myeloma cells (in log phase) were combined in a 5:1 ratio, and fusion was performed using polyethylene glycol (MW 1450 Hybri-Max; SigmaAldrich, Inc.). Fused cells were initially grown in nonselective full medium for 24 h, subsequently reconstituted in a methylcellulose-based hybridoma selection and cloning medium containing hypoxanthine, aminopterin, and thymidine (ClonaCell-HY Medium D; Stemcell, Inc.), and then grown for 10 to 12 days. Each cell colony was picked using a pipette tip, transferred onto a well in a 96-well plate containing 100 μl of hybridoma growth medium containing hypoxanthine and thymidine (ClonaCell-HY Medium E; Stemcell, Inc.), and further grown for 3 to 4 days. Supernatants from ~2,000 individual colonies were initially screened by enzyme-linked immunosorbent assay (ELISA) using baculovirus-expressed HAs of HK/68 and later rescreened by immunostaining on MDCK cells infected with Vic/11 cells as previously described (27).

Supernatant from hybridoma cultures producing MAb was harvested, clarified by low-speed centrifugation (30 min at 200 × *g*), and passed through a 0.22-μm-pore-size sterile filtration unit. The filtered supernatant was passed through a gravity flow column containing protein G-Sepharose 4 Fast Flow (GE Healthcare), washed with 150 ml of sterile 1× phosphate-buffered solution (PBS), and eluted with 45 ml of 0.1 M glycine-HCl (pH 2.9). The eluate was immediately neutralized with 5 ml of 2 M Tris-HCl buffer (pH 10). The antibody was concentrated using Amicon Ultra centrifugal filter units (30-kDa MWCO; Millipore, Inc.). MAb concentrations were quantified by using a NanoDrop apparatus with the extinction coefficient of 1.4.

CR8020 variable kappa light chain (GenBank accession no. JN093123.1) and heavy chain (GenBank accession no. JN093122.1) sequences were cloned into pFUSE2ss-CLIg-mK (Invivogen, Inc.) and pFUSE-CHIg-mG2a (Invivogen, Inc.), respectively. The MAb was produced recombinantly through transient transfection of 293Freestyle cells (Life Technologies, Inc.) of the corresponding heavy- and light-chain pFUSE plasmids with Polyethylenimine Max (Polysciences, Inc.). Cultures were spun down, and the supernatant was harvested at 6 days posttransfection and purified via a Protein G column (Millipore, Inc.). MAbs were concentrated with Amicon 30,000 MW filters (Millipore, Inc.). Purity was monitored under reducing/denaturing and nonreducing/nondenaturing conditions. Purified antibody was quantified as described above.

ELISA. Binding affinity of antibodies as determined by ELISA was previously described (27). Nunc Maxisorp 96-well plates were coated with 50 μl of purified baculovirus-expressed protein (2.5 μg/ml) or virus preparation (5 μg/ml) overnight at 4°C. After incubation, plates were washed twice with 0.1% Tween 20–1× PBS (TPBS) and blocked with 5% nonfat (NF) milk–1× PBS for 30 min at room temperature. Hybridoma supernatants or antibodies were incubated for 2 h at room temperature and washed thrice with 0.1% TPBS, and 100 μl of a goat anti-mouse IgG γ chain-specific antibody conjugated to horseradish peroxidase (HRP; Millipore, Inc.) was added at a dilution of 1:5,000. Plates were incubated at

TABLE 1 Binding of MAb 9H10 against group 2 HAs and HA variants[a]

Subtype	Year	Isolate	K_d (nM)	HA2							
				18	19	25	32	33	34	38	150
H3N8	1963	A/duck/Ukraine/1/1963	49	I	D	R	T	G	Q	L	E
H3N2	1968	A/HongKong/1/1968	7.5	I	D	R	T	G	Q	L	E
H3N2	1968	A/HongKong/1/1968 I18M	10	M	D	R	T	G	Q	L	E
H3N2	1968	A/HongKong/1/1968 D19N	23	I	N	R	T	G	Q	L	E
H3N2	1968	A/HongKong/1/1968 R25M	8500	I	D	M	T	G	Q	L	E
H3N2	1968	A/HongKong/1/1968 T32E	–	I	D	R	E	G	Q	L	E
H3N2	1968	A/HongKong/1/1968 T32I	10	I	D	R	I	G	Q	L	E
H3N2	1968	A/HongKong/1/1968 T32R	1900	I	D	R	R	G	Q	L	E
H3N2	1968	A/HongKong/1/1968 G33E	1900	I	D	R	T	E	Q	L	E
H3N2	1968	A/HongKong/1/1968 Q34R	–	I	D	R	T	G	R	L	E
H3N2	1968	A/HongKong/1/1968 Q34T	–	I	D	R	T	G	T	L	E
H3N2	1968	A/HongKong/1/1968 L38Y	6.2	I	D	R	T	G	Q	Y	E
H3N2	1968	A/HongKong/1/1968 E150A	5.6	I	D	R	T	G	Q	L	A
H3N2	1975	A/Victoria/3/1975	7.4	I	D	R	T	G	Q	L	G
H3N2	1979	A/Bangkok/1/1979	0.7	V	D	R	T	G	Q	L	G
H3N2	1986	A/Leningrad/360/1986	0.9	V	D	R	T	G	Q	L	G
H3N2	1989	A/Beijing/353/1989	0.8	V	D	R	T	G	Q	L	G
H3N2	1993	A/Shangdong/9/1993	0.6	V	D	R	T	G	Q	L	G
H3N2	1999	A/Panama/2007/1999	13	V	D	R	T	G	Q	L	G
H3N2	1999	A/Moscow/10/1999	16	M	D	R	T	G	Q	L	G
H3N2	2003	A/Wyoming/3/2003	0.6	V	D	R	T	G	Q	L	E
H3N2	2007	A/Brisbane/10/2007	1.5	V	D	R	I	G	Q	L	G
H3N2	2009	A/Perth/16/2009	153	V	D	R	R	G	Q	L	G
H3N2	2011	A/Victoria/361/2011	156	V	D	R	R	G	Q	L	G
H4N6	1956	A/duck/Czechoslovakia/1956	–	I	D	R	T	G	T	L	E
H7N7	2003	A/chicken/Netherlands/219/2003	–	I	D	R	E	G	T	Y	A
H7N9	2013	A/Shanghai/02/2013	–	I	D	R	E	G	T	Y	A
H10N7	1949	A/chicken/Germany/N/1949	15	V	D	R	T	G	Q	Y	E
H14N5	1982	A/mallard/Astrakhan/263/1982	–	I	D	R	T	G	T	L	E
H15N8	1979	A/shearwater/W. Austral./2576/1979	–	I	D	R	Q	G	T	Y	E
Consensus sequence				**V**	**D**	**R**	**T**	**G**	**Q**	**L**	**G**

[a] The binding affinity of MAb 9H10 with a panel of group 2 HA and HK/68 HA variants was measured by BLI. All numbered residues indicated are located in the HA2 region. Residues that differ from the group 2 consensus sequence are in highlighted in gray boxes.

37°C for 1 h and washed another three times with 0.1% TPBS before the addition of 100 μl of a soluble substrate, *o*-phenylenediamine dihydrochloride (Sigma-Aldrich, Inc.). The plates were read at 450 nm. All antibodies were diluted in 1% bovine serum albumin (BSA)–1× PBS. The mouse MAbs 12D1 (pan-H3) (24) and E10 (anti-M2; Center for Therapeutic Antibody Development at Icahn School of Medicine at Mount Sinai [CTAD]) were used as positive controls, while 6F12 (pan-H1) (27) and an anti-ankyrin antibody (ANK; CTAD) were used as negative controls. A nonlinear regression curve was generated using GraphPad Prism 4.0, and the 50% effective dose was calculated from the nonlinear curve.

pH-induced conformational change ELISA. Nunc Maxisorp 96-well plates were coated with purified preparations of HK/68 virus (5 μg/ml) overnight at 4°C. Plates were washed with 1× PBS twice and then incubated with appropriate pH-buffered solutions (15 mM citric acid, 150 mM NaCl; pH 7.0, 5.2, 5.0, 4.2, and 4.0) for 30 min at room temperature and then washed again with 1× PBS. Thereafter, a standard ELISA protocol was followed as described above.

***K_d* determination.** K_d (dissociation constant) values were determined by biolayer interferometry (BLI) using an Octet RED instrument (ForteBio, Inc.), as described below. Biotinylated HAs were loaded onto streptavidin-coated biosensors in 1× kinetics buffer (1× PBS [pH 7.4], 0.01% BSA, 0.002% Tween 20) for 180 s. For the measurement of k_{on}, the association of 9H10 Fab was measured for 180 s by exposing the sensors to four to six concentrations of Fab in 1× kinetics buffer. For the measurement of k_{off}, the dissociation of 9H10 Fab was measured for 180 s in 1× kinetics buffer. Experiments were performed at 30°C. The ratio of k_{off} to k_{on} determines the K_d.

Structure determination by negative-stain transmission electron microscopy (EM). Single-particle observations of HK/68 HA complexed with 9H10 Fab were used to compute volume maps as follows. Carbon-coated 400-mesh copper grids were glow-discharged with a Gatan Solaris plasma cleaner, treated with freshly diluted complexes, and negatively stained (2% uranyl formate). Micrographs were acquired at ×52,000 magnification on a Tecnai Spirit (accelerating voltage of 120 kV) with Leginon automation software (30). A Tietz charge-coupled device camera was used to acquire 283 micrographs (4,096 × 4,096 pixels, 2.05 Å/pixel) at an applied defocus of −1 μm. Single particles were automatically identified by using a difference-of-Gaussians algorithm implemented in the Appion package (31) and were analyzed in 64 × 64 pixel boxes after binning by a factor of 3. Reference-free class averages were derived from CL2D (32) and ISAC (33) and were manually edited to exclude noisy class averages. Initial volumes were calculated using the common lines algorithm in EMAN2 (34). Volumes were refined with the Sparx "ali3d.py" function (35). The final volume map was calculated from 4,791 particles with C3 symmetry applied. The map was interpreted with a homology model of Fab 9H10 (built with Swiss-Model [36]) using UCSF-Chimera (37). The correct enantiomorph was determined through consistency with the binding data (Table 1; see also Fig. 4A). Representative class averages and the resolution estimation by Fourier shell correlation (24.6 Å) are described in Fig. 4B and C. The volume map has been deposited as EMD-6077.

RBC fusion assay. The red blood cell (RBC) fusion assay was performed as described previously (24). Briefly, 100 μl of 2% turkey RBCs and 100 μl of Perth/09 virus were incubated on ice for 30 min. MAb 9H10 (at 100, 20, or 4 μg/ml) or a control IgG (ANK) was then added to the mixtures. The samples were spun down at 4,000 × *g* for 3 min, and the supernatant was aspirated. Next, 200 μl of a buffered solution (15 mM citric acid [pH 5.0], 150 mM NaCl) was added, and the mixture was incubated at 37°C for 30 min. The samples were spun at 4,000 × *g*, and the supernatant was harvested. Lysis of RBCs was measured by the presence of

NADPH (i.e., the optical density at 340 nm) in the supernatant released by lysed RBCs.

Egress assay. MDCK cells were first infected with a multiplicity of infection (MOI) of 5 of HK/68 or rVN/04. At 4 h postinfection, MAb 9H10 or control IgG (ANK) was added to the culture. At 8 h postinfection, supernatants from the cultures were harvested and spun down at 180 × *g* for 5 min to pellet the cellular debris. Nascent virus in the supernatant was assessed by using a hemagglutination assay as previously described (38).

Immunofluorescence. MDCK cells were infected at an MOI of 3 to 5 with HK/68, Scot/74, AL/81, BJ/92, Bris/07, Vic/11, rVN/04, SH/13, cH5/3, or cH7/3 for 12 to 16 h in the absence of trypsin. Cells were fixed with 0.5% paraformaldehyde (PFA)–1× PBS for 30 min at room temperature and blocked with 5% NF milk for an additional 30 min at room temperature. MAbs were diluted in 5% NF milk–1× PBS and then incubated at room temperature for 2 h at a final concentration of 5 μg/ml. The plates were then washed thrice with 1× PBS. A goat anti-mouse antibody conjugated to Alexa Fluor 488 (2 mg/ml; Life Technologies, Inc.) was used as a secondary antibody (1:1,000 in 5% NF-milk), followed by incubation at room temperature for 1 h. Images were taken by using an EVOS XL cell imaging system (Life Technologies, Inc.).

PRNA. A modified plaque reduction neutralization assay (PRNA) was described previously (24, 27). Briefly, dilutions (100 to 0.032 μg/ml) of antibodies were first preincubated with 80 to 100 PFU of virus for 1 h at room temperature on a shaker. The mixture was then used to infect a monolayer of MDCK cells in duplicate in a six-well plate format, followed by incubation at 37°C for 40 min with intermittent rocking. The agar overlay was supplemented with corresponding MAb dilutions. At 2 days postinfection (dpi), the monolayer was fixed with 4% PFA–1× PBS for 30 min and permeabilized with 0.5% Triton X-100 for 20 min. Cells were blocked with 5% NF milk–1× PBS for 30 min at room temperature, followed by incubation with polyclonal sera (1:500) or with 12D1 (5 μg/ml) for 1 h at room temperature. A goat anti-mouse IgG γ chain-specific antibody conjugated to HRP (Millipore, Inc.) was used as a secondary antibody, and plaques were subsequently visualized using TrueBlue peroxidase substrate (KPL, Inc.). A nonlinear curve was generated with GraphPad Prism 4.0, and the 50% inhibitory concentration (IC_{50}) was calculated from the curve.

Generation of *in vitro* escape mutants. Escape mutations were generated as previously described (27). Briefly, Scot/74 or Vic/11 virus was passaged 10 times (virus was passaged 1:10 to 1:100 every 2 days) on MDCK cells in 1× minimal essential medium, supplemented with 1 μg of TPCK (tolylsulfonyl phenylalanyl chloromethyl ketone)-treated trypsin/ml. Infection was started with an MOI of 0.1, and the concentration of MAb 9H10 was incrementally increased from 1 to 100 μg/ml from passages 1 to 10. Escape mutant cultures were performed in duplicate, and cultures with no antibodies were cultured in parallel to control for cell-specific adaptations. After the tenth passage, viral RNA was isolated, and the HA segment was sequenced from plaque-purified viruses. Ten sequences from Vic/11 and six sequences from Scot/74 escape cultures were sequenced and analyzed against wild-type sequences from the no-antibody control group. The HA segments were then cloned into a pCAGGS expression vector and used to transfect 293T cells. At 24 h posttransfection, the cells were fixed with 0.5% paraformaldehyde and blocked with 5% NF milk. MAbs 9H10, CR8020, and 6F12 were used at a concentration of 5 μg/ml, and a goat anti-mouse antibody conjugated to 488 (2 mg/ml; Millipore, Inc.) was used as a secondary antibody. Hyperimmune serum (diluted to 1:1,000) was used as a positive control. Immunofluorescence was used to determine MAb 9H10 binding as described above.

Animal studies. To assess the efficacy of MAb 9H10 in a preexposure regimen, 6- to 8-week-old female BALB/c mice (Jackson Laboratories, Inc.) were treated intraperitoneally with MAb 9H10 at 0.56, 1.67, 5, or 15 mg/kg or a mouse control IgG (ANK) at 15 mg/kg 2 h prior to an intranasal challenge of five 50% mouse lethal doses (mLD_{50}) of X-31 or X-79 virus. To assess the therapeutic efficacy, mice were initially challenged with five mLD_{50} of either X-31 or X-79 and were then administered 20 mg/kg of MAb 9H10 at 2, 3, 4, or 5 days postchallenge. All mice were monitored daily, and their weights were recorded until the end of a 2-week observation period. Death was defined as 25% body weight loss, and this threshold was used in both the pre- and postexposure experiments. All of the animal studies were conducted with the approval of the Icahn School of Medicine at Mount Sinai Institutional Animal Care and Use Committee (IACUC) protocol.

To determine viral load in the lungs, mice treated with 15 mg/kg of either MAb 9H10 or control IgG (ANK) were sacrificed at 3 and 6 dpi. Their lungs were harvested and homogenized (Fastprep-24; MP Biomedical) in 1 ml of 1× PBS. The lung homogenates were spun at 16,000 × *g* for 15 min to pellet tissue debris, and the supernatants were collected. Samples were stored at −80°C until titered by a plaque assay as previously described (27). GraphPad was used to calculate statistical significance between groups using a two-way analysis of variance analysis. A *P* value of <0.0001 (see Fig. 8) was considered statistically significant.

RESULTS

Generation of a stalk pan-H3 and H10 mouse MAb. We have previously reported on a pan-H3 HA MAb, 12D1, of which the epitope was mapped to near the N terminus of the long α-helix region of the stalk domain of HA (24). In the interest of elucidating conserved epitopes on the group 2 HA, we sought to generate MAbs against the conserved regions of the H3 HA stalk by using a strategy similar to one we had utilized previously (24, 27). In the present study, a mouse was sequentially immunized with sublethal doses of three divergent H3N2 viruses—rPhil/82, Vic/11, and HK/68—spanning 43 years. Hybridomas were initially screened against a purified preparation of baculovirus-expressed HK/68 HA and subsequently screened against Vic/11-infected MDCK cells.

Of the 2,000 hybridoma cells that were screened, we identified one hybridoma, 9H10, that secreted an antibody that bound to both the purified preparation of HK/68 HA protein and Vic/11-infected MDCK cells. To assess the breadth of binding that MAb 9H10 has for H3 HAs, we examined binding against a large panel of baculovirus-expressed HAs by ELISA (Fig. 1) and biolayer interferometry (BLI; Table 1). MAb 9H10 bound to all H3 HAs tested with high affinity, accommodating 48 years of antigenic drift from avian (1963) to human (1968 to 2011) H3 HAs (Fig. 1 and Table 1). We next wanted to determine whether MAb 9H10 would also bind to other group 2 influenza A virus subtypes (Fig. 2A to 2E and Table 1). Of the group 2 subtypes tested, MAb 9H10 bound only to H10 HAs (Fig. 2C and Table 1) with no detectable binding to H4 (Fig. 2A), H7 (Fig. 2B), H14 (Fig. 2D), and H15 (Fig. 2E) HAs at 100 μg/ml. As expected, MAb 9H10 did not bind any HAs from group 1 (Fig. 2F to H and Table 1).

Because partial denaturation may occur when proteins are coated onto hydrophobic surfaces of ELISA plates, we assessed MAb 9H10 binding to native HA expressed on the surfaces of infected cells. We infected MDCK cells with different viruses at an MOI of 3 to 5 overnight (~12 to 16 h) in the absence of trypsin to limit viral replication to a single cycle. The monolayers of MDCK cells were fixed with 0.5% paraformaldehyde without permeabilization. Immunofluorescence was then used to visualize binding of MAb 9H10 (at 5 μg/ml). We observed that MAb 9H10 bound evenly across the surface with no punctate staining on all H3- and H10-infected MDCK cells we tested, which suggested expression of HA glycoproteins on the cell surface (Fig. 3). However, no binding was seen on H7 (rSH/13)- and H5 (rVN/04)-infected cells (Fig. 3, bottom row), a finding consistent with the ELISA and BLI binding studies.

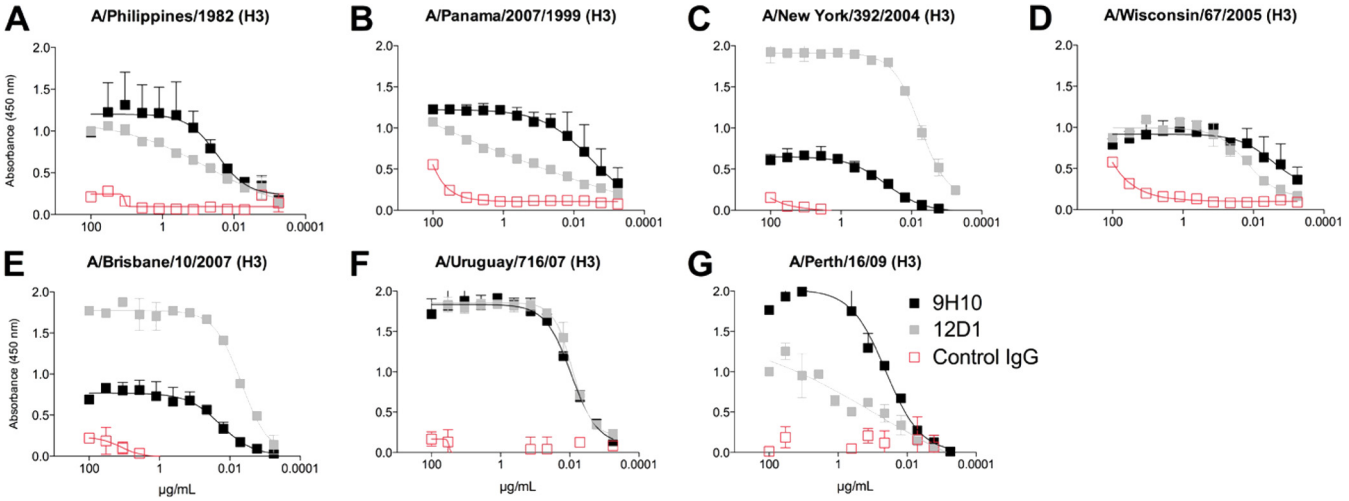

FIG 1 MAb 9H10 is a pan-H3 HA antibody. ELISA plates were coated with 50 μl of purified baculovirus-expressed HA (2.5 μg/ml) and incubated overnight at 4°C. MAb 9H10 (starting at 100 μg/ml) was diluted 3-fold and incubated at room temperature for 2 h. The plates were washed thrice with 0.1% PBST, and a goat anti-mouse IgG antibody conjugated to HRP was used as a secondary antibody. Plates were incubated at 37°C for 1 h and then washed thrice with 0.1% PBST. The HRP substrate *o*-phenylenediamine dihydrochloride was used, and plates were read at 450 nm. A control IgG (an anti-ankyrin MAb, ANK) was used as a negative control, and MAb 12D1, a previously identified pan-H3 MAb, was used as a positive control. A nonlinear curved was generated with GraphPad Prism 4.0.

To determine whether MAb 9H10 targets the HA stalk, we utilized recombinant influenza A viruses expressing chimeric HAs. The modular structure of chimeric HAs allows for the combinations of globular head domains and the stalk regions from different strains and/or subtypes of influenza viruses (39), which subsequently enables identification of head- or stalk-directed antibodies (40). MAb 9H10 bound to both cH5/3 (chimeric H5 head with H3 stalk)- and cH7/3 (chimeric H7 head with H3 stalk)-infected cells, suggesting that the antibody binds the HA stalk (Fig. 3, bottom row). Moreover, MAb 9H10 competes with the anti-stalk MAb CR8043 for binding to the HA but not with the anti-head MAb F045-092 (13) (Fig. 4A). Finally, a negative-stain electron microscopy (EM) reconstruction of the 9H10 Fab in complex with HK/68 (H3) HA revealed that the antibody binds at the base of the HA stalk (Fig. 4B to D).

MAb 9H10 has broadly neutralizing activity against H3 and H10 viruses. We next evaluated whether broad reactivity would correlate to broad neutralizing activity. Since stalk antibodies do not have HAI activity (23, 27), we investigated neutralization by using a plaque reduction neutralization assay. We show that MAb 9H10 neutralized 10 H3N2 viruses representing a span of 43 years with various efficacies, as well as one H10 virus (Table 2). In agreement with the binding studies, MAb 9H10 did not neutralize H1, H4, H5, and H7 viruses.

MAb 9H10 binding specificities and structural comparison to CR8020 and CR8043. To map the epitope of MAb 9H10, we tested the binding of the antibody to a series of HA mutants that encompass natural variations, as well as escape mutants for the previously characterized human stalk MAbs CR8020 and CR8043 (22, 23). The mutants that abrogated binding by MAb 9H10 were

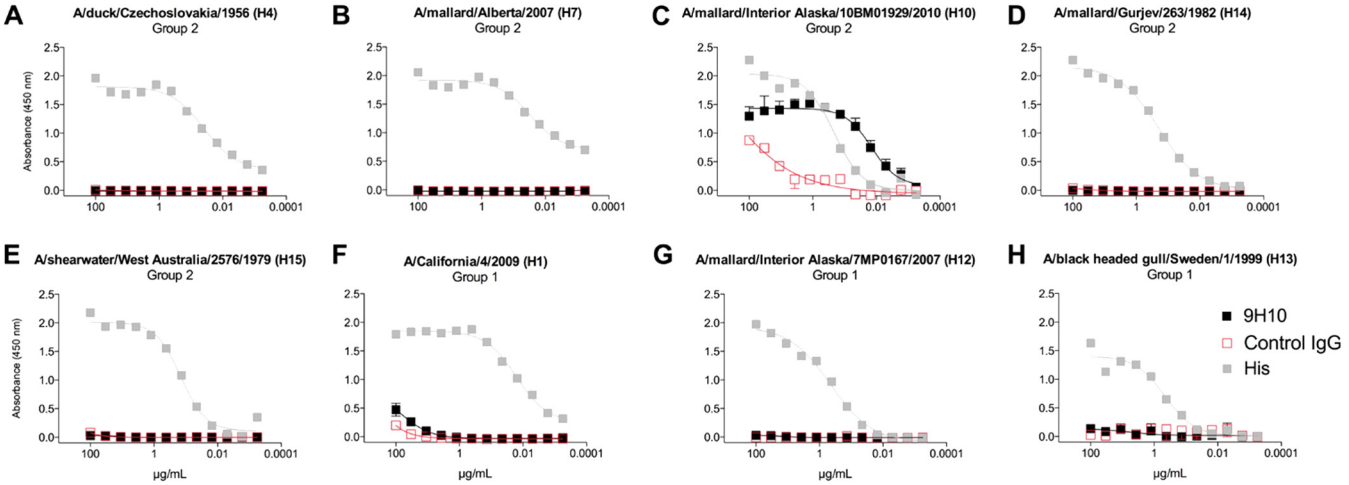

FIG 2 MAb 9H10 also binds to H10 HA but not to other group 2 or group 1 HAs. ELISA plates were coated with purified HA from other group 2 HAs (A to E) and group 1 HAs (F to H) as described previously. MAb 9H10 was used at a starting concentration of 100 μg/ml. An anti-histidine polyclonal (His) antibody and control IgG (ANK) were used as positive and negative controls, respectively. A standard ELISA protocol was followed as described above.

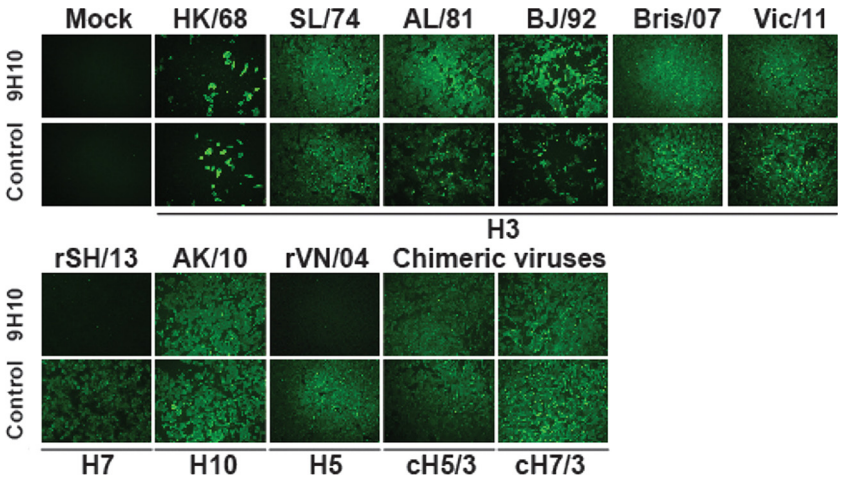

FIG 3 MAb 9H10 binds to the stalk domain of H3 HA. MDCK cells were infected with the indicated influenza viruses at an MOI of 3 to 5 for 12 to 16 h without trypsin. The cells were fixed with 0.5% paraformaldehyde and blocked with 5% nonfat (NF) milk. MAb 9H10 was used at a concentration of 5 μg/ml, and a goat anti-mouse antibody conjugated to Alexa Fluor 488 was used as a secondary antibody. Recombinant chimeric viruses cH5/3 and cH7/3 express HAs that have the globular head domain of H5 (VN/04) and H7 (SH/13), respectively, with the stalk domain of an H3 (Perth/09) HA. An MAb directed against the M2 protein (Control) served as a positive infection control.

Arg25Met, Thr32Glu, Gln34Arg, and Gln34Thr on the HA2 subunit (Table 1). Other HA2 variants that severely weakened the interaction had point mutations at Thr32Arg and Gly33Glu (Table 1). These residues are located on the HA stem on the β-sheet of HA2 preceding the short α-helix (Fig. 5A). Among these residues, the identity of position 34 appears to separate binders (Gln34) from nonbinders (Thr34), just as for CR8043 (22). Accordingly, Thr34 is highly conserved in the H4, H7, H14, and H15 subtypes,

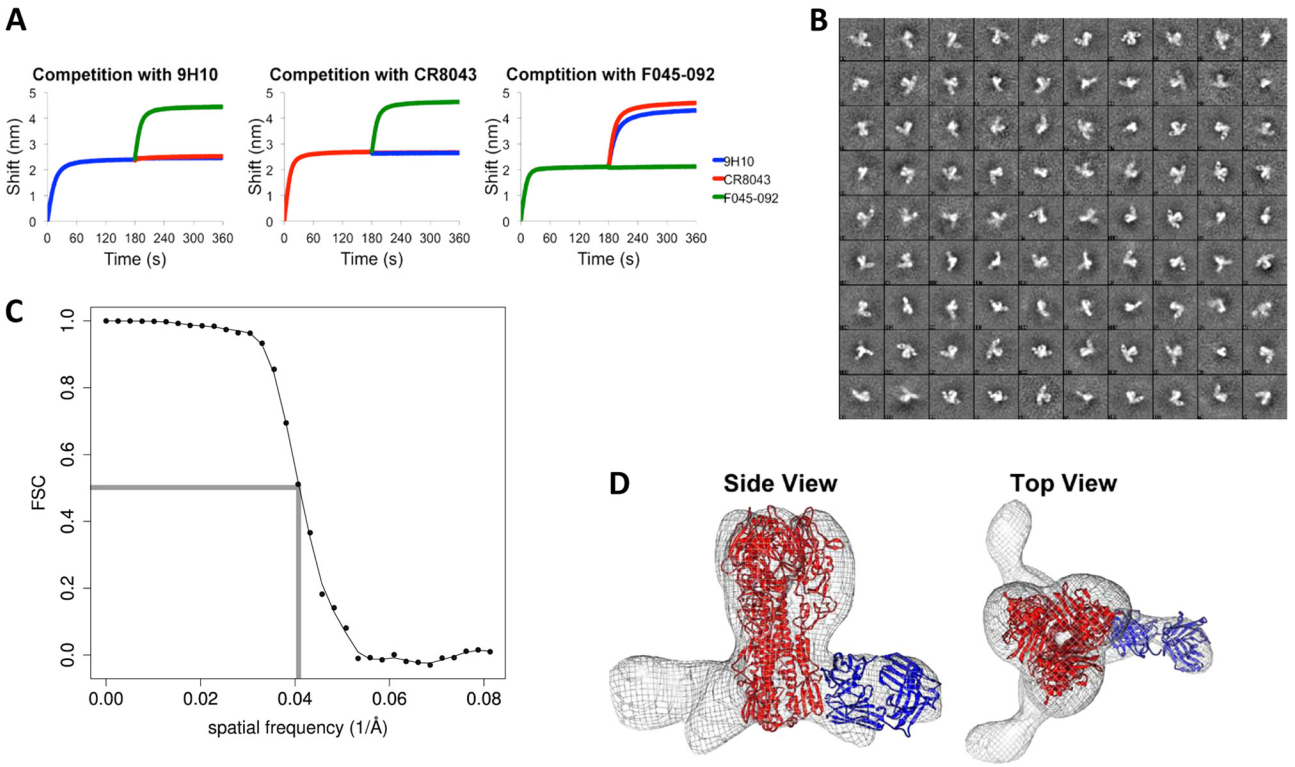

FIG 4 MAb 9H10 binds to the membrane-proximal region of the HA stalk. (A) Antibody binding competition of MAb 9H10, CR8043 (stalk MAb), or F045-092 (head MAb) with immobilized A/Hong Kong/1/1968 (H3) HA presaturated with MAb 9H10, CR8043, or F045-092, as measured by BLI. (B) Single-particle analysis by electron microscopy affords reference-free class averages showing the negatively stained complexes. These class averages were used to initiate volume reconstruction by common lines. (C) Fourier shell correlation analysis showing the volume map's resolution to be less than ~25 Å. (D) Volume reconstruction of Fab 9H10 in complex with the A/Hong Kong/1/1968 (H3) HA. The crystal structure of A/Hong Kong/1/1968 (H3) HA (red) and a homology model of 9H10 (blue) are docked into the EM map (gray mesh).

TABLE 2 MAb 9H10 has broad neutralizing activity against H3 and H10 viruses[a]

Group and subtype	Isolate	IC_{50} (μg/ml)
Group 1		
H1N1	A/California/4/2009*	>100
H5N1	A/Vietnam/1203/2004*	>100
Group 2		
H3N2	A/Hong Kong/1/1968 (X-31)*	1.49
H3N2	A/Scotland/840/1974	0.09
H3N2	A/Victoria/3/1975	0.74
H3N2	A/Philippines/2/1982 (X-79)*	0.23
H3N2	A/Beijing/47/1992	0.08
H3N2	A/Panama/2007/1999	0.14
H3N2	A/Wyoming/3/2003	0.05
H3N2	A/Brisbane/10/2007	0.03
H3N2	A/Perth/16/2007	7.17
H3N2	A/Victoria/361/2011	2.44
H4N6	A/duck/Czechoslovakia/1956	>100
H7N1	A/rhea/North Carolina/1993	>100
H10N7	A/mallard/Interior Alaska/10BM01929/2010	2.89

[a] The IC_{50} of MAb 9H10 was calculated from the nonlinear curve generated from the plaque reduction neutralization assay data against several subtypes of the influenza A virus group 1 and group 2. Samples with no neutralization are indicated by ">100" (the highest tested MAb concentration). *, Reassortant viruses with internal proteins of PR/8 (H1N1) expressing the HA and NA of the respective isolate.

likely accounting for the inability of MAbs 9H10 and CR8043 to target these subtypes. Although antibodies 9H10, CR8020, and CR8043 appear to share an overlapping epitope on the HA, as determined by comparison of the 9H10 EM reconstruction here to previous EM and crystal structures of CR8020 and CR8043 (22, 23), their sensitivities to mutations are distinct, which may be explained by their slightly different approach angles to the HA (Fig. 5B).

Generation of *in vitro* escape mutants against MAb 9H10. The generation of escape mutants allows for the identification of amino acid residues that are critical in the formation of an antibody epitope. We generated escape mutants of two divergent H3 viruses: Scot/74 and Vic/11. Each virus was passed in MDCK cells 10 times in the presence of MAb 9H10, and the escape mutants were plaque purified. The sequences of the HA segments of plaque-purified viruses reveal point mutations in the HA2 domain: one was found in Scot/74 (Arg25Met), while two were found in Vic/11 (Asp19Asn and Thr107Ala) (Fig. 6A). The wild-type and mutant HA segments were subcloned into an expression vector, and binding of MAbs was assessed by immunofluorescence in transfected 293T cells. A point mutation at position Arg25Met on the Scot/74 HA2 (emScot/74) resulted in loss of binding to MAb 9H10 (Fig. 6A and B). Similarly, we observed that residue changes at positions Asp19Asn/Thr107Ala on the Vic/11 HA (emVic/11) ablated binding of MAb 9H10 (Fig. 6B). A previously reported stalk human MAb, CR8020, also did not bind to the emVic/11 HA, which possesses the Asp19Asn/Thr107Ala point mutations (Fig. 6B) (23). MAb CR8020, however, was still able to bind to the emScot/74 HA (Arg25Met), albeit with lower efficacy. A stalk antibody, 6F12 (27), against group 1 HAs that was used as a control IgG did not bind to any of the group 2 HAs.

Mechanisms of inhibition. The influenza virus genome enters the host cytoplasm through an HA-mediated membrane fusion process. Acidification of the endosome causes a conformational change of the HA, which allows for the fusion of the viral and endosomal membranes. Stalk antibodies are thought to bind and lock the HA in its prefusion conformation to prevent the HA from undergoing drastic conformational changes during acidification (23, 27). To reinforce the interpretations of the EM data (Fig. 5), we further examined how MAb 9H10 bound to the HA in its prefusion native conformation by assessing the pH dependence of HK/68 virus binding by ELISA. MAb 9H10 maintained binding when the HK/68 HA was presubjected to pH 7.0 to 5.0 but appreciably lost ability to bind to HA preexposed to pH 4.2 and 4.0 (Fig. 7A). In contrast, binding of the anti-head MAb XY102 remained the same irrespective of the exposure of the HA to a wide range of pH values (Fig. 7B). We therefore conclude that the epitope of MAb 9H10 is present in the prefusion conformation of HA at neutral pH but is gradually ablated as the pH is decreased.

We subsequently wanted to assess whether binding to the native prefusion conformation of HA would prevent fusion in an *in vitro* assay. Turkey red blood cells (RBCs) and Perth/09 virus were initially preincubated with serial dilutions (100 to 4 μg/ml) of MAb and then exposed to a low-pH buffer (pH 5). Fusion was determined by measuring the release of NADPH through RBC lysis. We observed that MAb 9H10 inhibited RBC lysis in a dose-dependent manner, with no inhibition of RBC lysis in the IgG and null MAb controls (Fig. 7C).

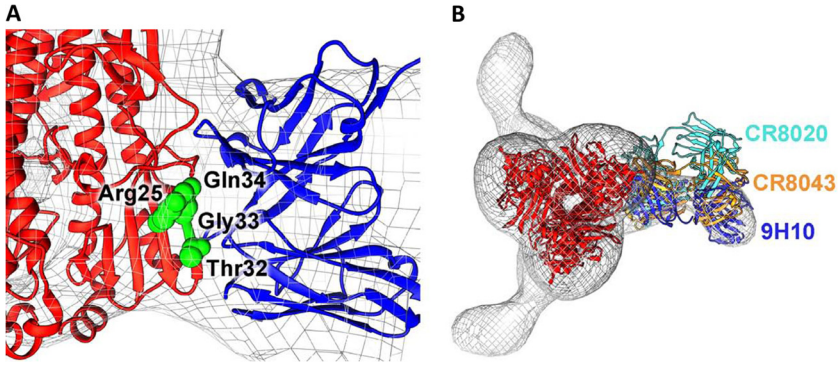

FIG 5 Key HA residues involved in binding. (A) Closeup view of the HA (red) and 9H10 (blue) interface, depicting the 9H10-sensitive HA2 residues 25, 32, 33, and 34 (green spheres) (22, 23). (B) Comparison of the approach angles of 9H10 (blue), CR8020 (cyan), and CR8043 (orange) to the HA (red).

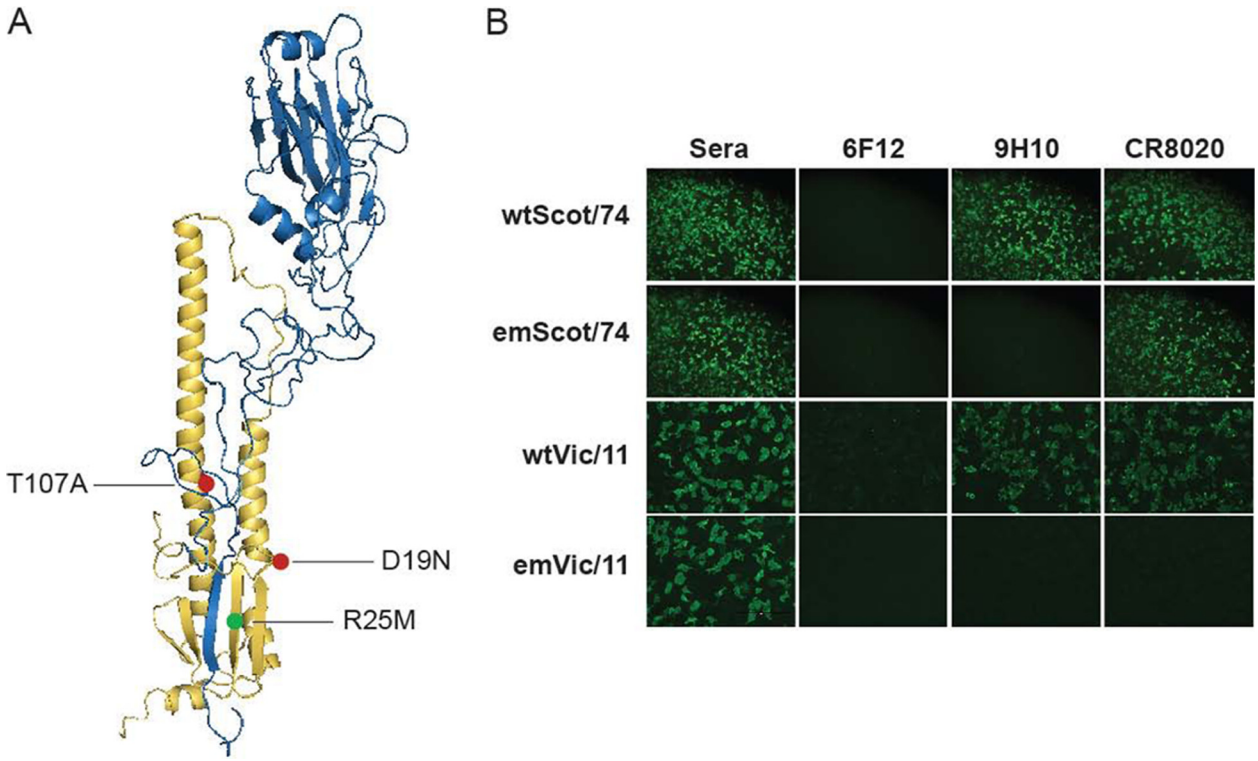

FIG 6 Binding analysis of escape mutants generated against two divergent H3N2 viruses. An escape mutant generated against Scot/74 (emScot/74) revealed one point mutation (R25M) in the HA2 domain, while an escape mutant against Vic/11 (emVic/11) had two point mutations (D19N and T107A). (A) An H3 HA monomer depicted using PyMOL shows the location of the point mutations found on emScot/74 HA (green) and emVic/11 HA (red), where HA1 is indicated in blue and the HA2 is indicated in yellow. The point mutation R25M (green) is located in the middle of the beta-sheet of the HA2 domain (yellow) of Scot/74 HA. The D19N (red) residue change is located at the elbow of the fusion peptide, while the T107A (red) resides in the middle of the long α-helix facing the short α-helix of HA2 (yellow) of Vic/11 HA. (B) 293T cells were transfected with wild-type or escape mutant HA and fixed at 24 h posttransfection. Reactivity was assessed by immunofluorescence using MAb 9H10 or MAb CR8020 (5 μg/ml). Infected mouse serum was used as a positive control, and a pan-H1 stalk MAb, 6F12 (5 μg/ml), was used as a negative control.

Lastly, we wanted to determine whether a stalk MAb has any effect on the late stage of the viral replication cycle. MDCK cells were initially infected with an MOI of 5 and, at 4 hpi, MAb 9H10 or control IgG (ANK) was added to the cultures. At 8 hpi, the supernatants were harvested, and the virus titer as measured by a hemagglutination assay was performed. At 100 μg/ml, MAb 9H10 prevented detectable nascent virus in the supernatants of H3-infected cells. Decreasing the amount of MAb 9H10 to 20 and 4 μg/ml increased the virus titers to 1 and 32 hemagglutination units (HAU), respectively (Fig. 7D). The control IgG (ANK) and null antibody groups did not prevent viral egress, and both had virus titers of 128 HAU at 8 hpi. As expected, MAb 9H10 did not prevent viral egress of an H5 (rVN/04) virus since all groups (MAb 9H10, control IgG, and null MAb) gave virus titers of 64 HAU (Fig. 7E). We thus conclude that MAb 9H10 can prevent viral egress of an H3 virus in a dose-dependent manner at 8 hpi when the antibody is added at 4 hpi.

MAb 9H10 has *in vivo* efficacy against two mouse-adapted H3 viruses in a preexposure regimen. We next assessed whether MAb 9H10 can protect mice from disease in a preexposure prophylaxis regimen against two mouse-adapted H3N2 viruses: X-31 and X-79. Groups of five mice were administered MAb 9H10, a control IgG (ANK) or 1× PBS intraperitoneally 2 h before being challenged intranasally with five mLD_{50} of either X-31 or X-79. Mice were weighed daily and sacrificed if they lost 25% of their original bodyweight. Mice pretreated with 5 to 15 mg/kg of MAb 9H10 transiently lost 5 to 10% of their body weight from 4 to 12 dpi when challenged with X-31 (Fig. 8A), a reassortant virus that expresses the HA and NA of the pandemic strain A/Hong Kong/1/1968 (H3N2). Mice that received 1.67 mg/kg of MAb 9H10 lost the most weight, losing a little less than 20% of their body weight, while the mice from the 0.56 mg/kg group all succumbed to disease by day 8 postchallenge. As expected, mice treated with the control IgG (ANK) or PBS gradually lost weight starting from day 3 postchallenge and were eventually euthanized or succumbed to disease by days 7 and 8 postchallenge. Against X-79, a reassortant virus that expresses the HA and NA of Phil/82 (H3N2), pretreatment with MAb 9H10 provided mice that received 1.67 to 15 mg/kg of MAb 9H10 full protection against death. Mice that received 0.56 mg/kg were partially protected from death with a 50% survival rate (Fig. 8B). A closer look at the mouse model showed that administration of MAb 9H10 significantly decreased viral lung titers by 1.5 and 4 logs against X-31 on days 3 and 6 postinfection, respectively (Fig. 8C). Against X-79, MAb 9H10 decreased viral lung titers by 1.5 log units on day 3 postinfection to undetectable levels on day 6 postinfection compared to the IgG control group (ANK) (Fig. 8D). We have thus demonstrated that the broad *in vitro* binding and neutralizing profile of MAb 9H10 also extends to the mouse model against two divergent mouse-adapted H3 viruses.

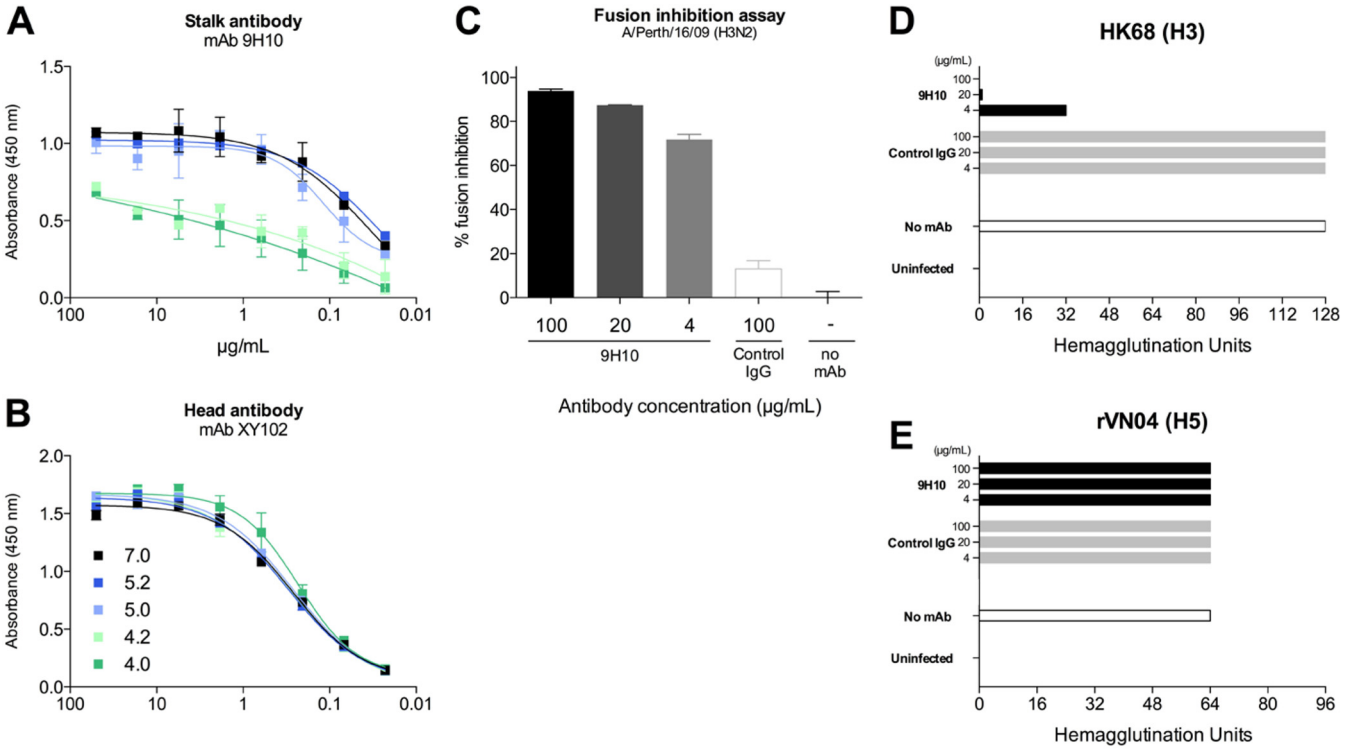

FIG 7 Mechanisms of inhibition of MAb 9H10. MAb 9H10 loses binding to HA at low pH. A purified preparation of HK/68 virus (5 μg/ml) was coated onto ELISA plates and exposed to pH-buffered solutions (pH 7.0, 5.2, 5.0, 4.2, and 4.0). Stalk-specific MAb 9H10 (A) or head-specific XY102 (B) starting at 100 μg/ml was used, and a standard ELISA was performed as previously described (27). MAb 9H10 inhibits fusion of HA envelope and RBC membrane. (C) MAb 9H10 was incubated with Perth/09 virus on ice 30 min. Fusion was induced by exposure to a low pH (5.0) buffer at 37°C for 30 min, and hemolysis was measured based on the release of NADPH in the supernatant at 340 nm. MAb 9H10 inhibits the budding of nascent H3 virus at 8 hpi. MDCK cells were infected with HK/68 (H3) (D) or rVN/04 (H5) (E) with an MOI of 5. At 8 hpi, the supernatants were harvested, and the virus titer was assessed by using a hemagglutination assay. The control IgG used was ANK as in previous experiments.

Postexposure administration of MAb 9H10 also protects mice from disease and death. To utilize a more stringent and realistic scenario, we first infected mice with five mLD_{50} of either X-31 or X-79 and, at 2, 3, 4, and 5 days postchallenge, 20 mg/kg of MAb 9H10 or a control antibody (ANK) was then administered intraperitoneally. Mice were weighed daily and monitored for any clinical signs of disease. Administration of MAb 9H10 at 2 and 3 dpi provided 80% protection from mortality against X-31 but with at least 20% body weight loss. Moreover, treatment at 4 and 5 dpi did not prevent disease or death and was comparable to the control group (Fig. 9A). However, MAb 9H10 provided better protection against X-79, similar to what was seen in the preexposure experiment. Treatment with MAb 9H10 at days 2 and 3 postchallenge provided 100% survival with a transient 10% weight loss, while treatment on day 4 postchallenge resulted in an 80% survival. Remarkably, the group treated at 5 days postchallenge resulted in a 20% survival, albeit with substantial weight loss.

DISCUSSION

The characterization of antibodies directed against the stalk domain of the influenza virus HA has yielded a wealth of information regarding the types of antibodies that can be elicited against influenza virus and the mechanisms by which this class of antibodies can inhibit viral replication (41). Stalk-directed antibodies are notable in that all are reactive against divergent influenza viruses, with some antibodies exhibiting broadly neutralizing activity across several subtypes, phylogenetic groups, or genera.

In the present study, we generated a mouse MAb that has a broad binding profile against H3 and H10 HAs tested by ELISA, immunofluorescence, and BLI. The broad binding profiles observed positively correlated with broad neutralization, demonstrating that MAb 9H10 is a pan-H3 and an H10 neutralizing antibody. In the animal model, MAb 9H10 protects mice from two divergent mouse-adapted H3N2 viruses (X-31 and X-79) in a preexposure challenge regimen. Protection, however, was strain dependent: a dose of 1.67 mg/kg (33 μg/animal) of MAb 9H10 provided 100% protection against X-31, whereas a dose as low as 0.56 mg/kg (11 μg/animal) can still provide 50% protection against X-79. Of note, the *in vivo* IC_{50}s of 9H10 against X-31 and X-79 were determined to be 3.9 and 1.6 mg/kg, respectively, which represents an ~2.4-fold difference. Interestingly, the IC_{50} of MAb 9H10 against X-79 (0.23 μg/ml) is ~6-fold better than against X-31 (1.49 μg/ml) in a plaque reduction assay, a finding which is in agreement with the better protection against the X-79 challenge *in vivo*. Although there is a difference between the *in vitro* and *in vivo* IC_{50}, our data suggest that our *in vitro* assay can predict the relative *in vivo* efficacy of an antibody. Furthermore, protection from weight loss and death is dependent upon viral clearance from the lungs. Mice treated with MAb 9H10 had a 10-fold smaller amount of virus at 3 dpi and an almost undetectable amount of virus in the lungs at 6 dpi compared to the control group. When

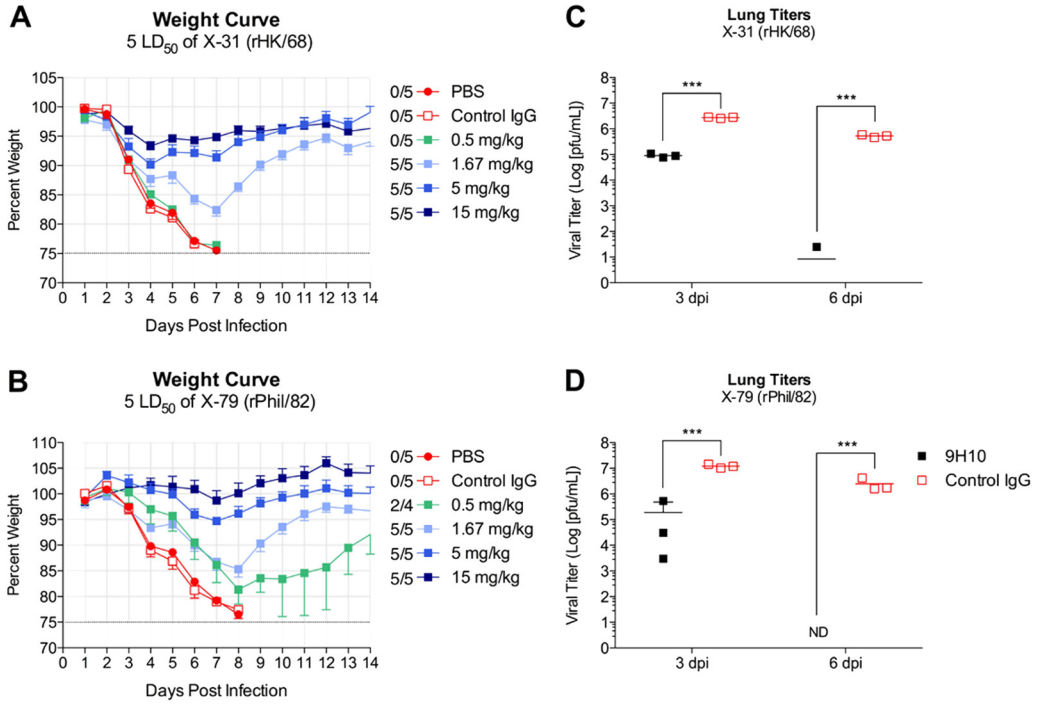

FIG 8 MAb 9H10 shows preexposure prophylactic activity against divergent H3N2 viruses *in vivo*. Mice were first administered with 0.5, 1.67, 5.0, and 15 mg/kg of MAb 9H10 intraperitoneally and challenged with five mLD_{50} of X-31 (rHK/68) (A) or X-79 (rPhil/82) (B) 2 h later. PBS- or control IgG (ANK)-treated mice were used as negative controls. Mice were monitored daily, and their weights were recorded for 14 days. Viral lung titers were assessed at 3 and 6 dpi in X-31 (rHK/68) (C)- and X-79 (rPhil/82) (D)-challenged mice initially treated with 15 mg/kg of MAb 9H10 or control IgG (ANK). ND, none detected; ***, $P > 0.0001$.

the antibody was administered after a lethal challenge, MAb 9H10 also provided better protection against X-79 compared to X-31. In fact, mice administered with MAb 9H10 4 and 5 days after X-79 challenge still gave partial protection (80 and 20%, respectively), albeit with greater weight loss when the MAB was administered at 2 and 3 dpi. Nonetheless, this result has great implications in the practical use of a MAb as an antiviral therapeutic. Studies have suggested that treatment with neuraminidase inhibitors such as zanamavir or oseltamivir exerts their optimum effects ~48 h after symptom onset in humans (42, 43). The findings that MAb 9H10 and other stalk antibodies can minimize morbidity and mortality in mice when administered at up to 3 to 5 dpi has great possibilities.

An influenza A virus particle is internalized into a host cell in a two-step process. Attachment of the HA via its sialic acid receptor allows the viral particle to be endocytosed where it is acidified within the endosome. Acidification induces a conformational change in the HA, facilitating the fusion of the viral and the endosomal membranes, thereby releasing the viral RNP into the cytoplasm. Unlike antibodies that target the globular head, which typically possess HAI activity, stalk antibodies do not prevent the binding interaction between HA and sialic acid. Instead, stalk antibodies are thought to stabilize the prefusion conformation of HA by binding and thus preventing the fusion of the viral and the endosomal membranes (44–46). We observed that MAb 9H10 gradually lost binding affinity as the HA was preexposed to low pH. More importantly, we show that the binding of MAb 9H10 to HA is functionally significant by preventing HA from undergoing

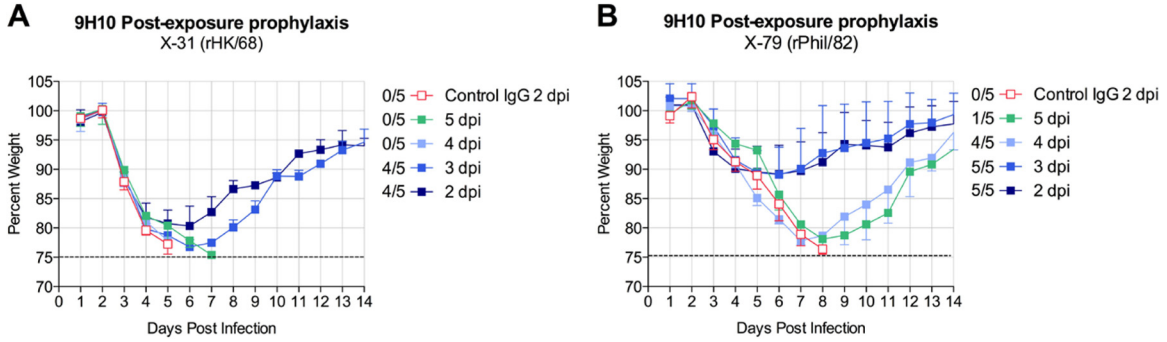

FIG 9 MAb 9H10 has therapeutic efficacy *in vivo*. Mice were first challenged with five mLD_{50} of X-31 (rHK/68) (A) or X-79 (rPhil/82) (B) and at 2, 3, 4 or 5 dpi, administered with 20 mg/kg of MAb 9H10 intraperitoneally. Control IgG (ANK) was administered only at 2 dpi. Mice were weighed daily and monitored for signs of disease.

conformational change, as demonstrated in an RBC fusion assay. The result highlights a common characteristic among stalk antibodies in their ability to prevent the fusion of viral and endosomal compartments in the early stage of infection. In the late phase of infection, we demonstrated that MAb 9H10 could disrupt viral egress in a dose-dependent manner against H3, in contrast to what others have previously reported that suggest that stalk antibodies do not inhibit viral egress (47). In our experimental condition, we added the MAb at 4 hpi to ensure that MAb 9H10 does not inhibit entry and measured viral egress after a one-step replication cycle (8 hpi). Examination of viral egress at 18 hpi or later time points, which is after several replication cycles, may confound the result and account for the different finding.

A comparison of the EM reconstructions of group 2 stalk antibodies bound to the HA suggest that the binding footprint of MAb 9H10 is similar to that of MAbs CR8020 and CR8043. Moreover, a more detailed analysis reveals that MAbs CR8043 and 9H10 have a similar angle of approach to their respective epitopes (Fig. 5B). In fact, the selection of the escape mutant generated against Scot/74 with MAb 9H10 is the same residue (Arg25Met) in the HA2 region as that generated with MAb CR8043 against HK/68. In contrast, MAb CR8020 still binds moderately to the Scot/74 escape mutant (Arg25Met), emphasizing differences in residues that are important for binding. It must be noted, however, that broadly neutralizing antibodies, such as MAb 9H10, may exert different pressures against other H3 strains. Thus, against a more recent H3 strain (Vic/11), antibody pressure selected for escape mutants that had two point mutations in the HA2 domain, Asp19Asn and Thr107Ala. A point mutation at Asp19Asn correlates with lower binding affinity and a loss of *in vitro* neutralization by MAb CR8020 as previously reported (23). It is interesting, however, that the point mutation, Thr107Ala, is not found on the surface of the epitope and does not participate in direct binding with MAb 9H10. Rather, position Thr107 is located inside the core of the trimeric HA, facing the internal surface of the short α-helix.

As increasing numbers of broadly neutralizing stalk antibodies are described, a more exhaustive map of the location of conserved epitopes can be established. Structural analyses of several broadly neutralizing MAbs (e.g., CR6261 and F10) against group 1 (H1 and H5) subtypes show that binding is centered around the short α-helix of HA2 with some involvement of residues on the N-terminal portion of HA1 (15, 18). Notably, the manner by which binding is achieved is dependent upon a conformationally intact prefusion HA trimer (28). Examination of two group 2 binding MAbs, CR8020 and CR8043, revealed that the fusion peptide and the β-sheet are involved in the formation of the epitope located at the base of the stalk of HA2 (22, 23). Thus, the epitope of group 2-specific antibodies CR8020 and CR8043 is markedly lower down the stalk domain compared to the epitopes of the group 1-specific antibodies CR6261 (18) and F10 (15). An overall observation of the spatial relationship between the conserved epitopes of group 1 versus group 2 binders suggests that the conserved epitopes of group 1 subtypes are centered around a hydrophobic groove between helices in the middle of the HA stalk. The conserved epitopes of group 2 binders, on the other hand, have thus far been shown to be at the base of the HA stem. Here, we show that MAb 9H10 maps to a similar location on the HA2 as CR8020 and CR8043. Furthermore, structural analyses reveal that although CR8020, CR8043, and 9H10 all appear to have overlapping binding footprints on the base of the HA, there are subtle differences that result in different binding and neutralization profiles.

Postexposure experiments in the mouse model demonstrate that stalk antibodies can be used as potential antiviral therapeutics. More importantly, however, they are useful in highlighting prospective targets for broad-spectrum anti-influenza therapies and vaccines. In addition to seasonal influenza virus epidemics, it is evident from recent reports that outbreaks of variant H3N2 viruses and sporadic zoonotic transmissions of other group 2 viruses (e.g., H3N8, H10N8, and H7N9) are always a cause for concern (48–51). With these ever-present threats to public health, the discovery and characterization of conserved epitopes in influenza virus would allow for better design of therapeutics and vaccines that would afford broad coverage.

ACKNOWLEDGMENTS

We thank Ariana Hirsh for excellent technical support and Jonathan Runstadler from the Department of Biological Engineering at Massachusetts Institute of Technology for the H10N7 isolate.

F.K. was supported by an Erwin Schrödinger fellowship (J3232) from the Austrian Science Fund. This study was partially supported by Centers for Excellence for Influenza Research and Surveillance grant HHSN266200700010C (P.P.) and by National Institutes of Health grants U19 AI109946 (P. P.) and R56 AI099275 (I.A.W. and A.B.W.).

REFERENCES

1. **World Health Organization.** 2014. Factsheet 211: influenza. World Health Organization, Geneva, Switzerland.
2. **Salzberg S.** 2008. The contents of the syringe. Nature **454:**160–161. http://dx.doi.org/10.1038/454160a.
3. **Gerdil C.** 2003. The annual production cycle for influenza vaccine. Vaccine **21:**1776–1779. http://dx.doi.org/10.1016/S0264-410X(03)00071-9.
4. **Bright RA, Shay DK, Shu B, Cox NJ, Klimov AI.** 2006. Adamantane resistance among influenza A viruses isolated early during the 2005-2006 influenza season in the United States. JAMA **295:**891–894. http://dx.doi.org/10.1001/jama.295.8.joc60020.
5. **Hobson D, Curry RL, Beare AS, Ward-Gardner A.** 1972. The role of serum haemagglutination-inhibiting antibody in protection against challenge infection with influenza A2 and B viruses. J. Hyg. **70:**767–777. http://dx.doi.org/10.1017/S0022172400022610.
6. **Coudeville L, Bailleux F, Riche B, Megas F, Andre P, Ecochard R.** 2010. Relationship between haemagglutination-inhibiting antibody titres and clinical protection against influenza: development and application of a Bayesian random-effects model. BMC Med. Res. Method. **10:**18. http://dx.doi.org/10.1186/1471-2288-10-18.
7. **Whittle JRR, Zhang R, Khurana S, King LR, Manischewitz J, Golding H, Dormitzer PR, Haynes BF, Walter EB, Moody MA, Kepler TB, Liao H-X, Harrison SC.** 2011. Broadly neutralizing human antibody that recognizes the receptor-binding pocket of influenza virus hemagglutinin. Proc. Natl. Acad. Sci. U. S. A. **108:**14216–14221. http://dx.doi.org/10.1073/pnas.1111497108.
8. **Lee PS, Yoshida R, Ekiert DC, Sakai N, Suzuki Y, Takada A, Wilson IA.** 2012. Heterosubtypic antibody recognition of the influenza virus hemagglutinin receptor binding site enhanced by avidity. Proc. Natl. Acad. Sci. U. S. A. **109:**17040–17045. http://dx.doi.org/10.1073/pnas.1212371109.
9. **Ekiert DC, Kashyap AK, Steel J, Rubrum A, Bhabha G, Khayat R, Lee JH, Dillon MA, O'Neil RE, Faynboym AM, Horowitz M, Horowitz L, Ward AB, Palese P, Webby R, Lerner RA, Bhatt RR, Wilson IA.** 2013. Cross-neutralization of influenza A viruses mediated by a single antibody loop. Nature **488:**526–532. http://dx.doi.org/10.1038/nature11414.
10. **Schmidt AG, Xu H, Khan AR, O'Donnell T, Khurana S, King LR, Manischewitz J, Golding H, Suphaphiphat P, Carfi A, Settembre EC, Dormitzer PR, Kepler TB, Zhang R, Moody MA, Haynes BF, Liao H-X, Shaw DE, Harrison SC.** 2013. Preconfiguration of the antigen-binding site during affinity maturation of a broadly neutralizing influenza virus antibody. Proc. Natl. Acad. Sci. U. S. A. **110:**264–269. http://dx.doi.org/10.1073/pnas.1218256109.
11. **Xu R, Krause JC, McBride R, Paulson JC, Crowe JE, Wilson IA.** 2013.

A recurring motif for antibody recognition of the receptor-binding site of influenza hemagglutinin. Nat. Struct. Mol. Biol. **20:**363–370. http://dx.doi.org/10.1038/nsmb.2500.

12. **Hong M, Lee PS, Hoffman RMB, Zhu X, Krause JC, Laursen NS, Yoon SI, Song L, Tussey L, Crowe JE, Ward AB, Wilson IA.** 2013. Antibody recognition of the pandemic H1N1 influenza virus hemagglutinin receptor binding site. J. Virol. **87:**12471–12480. http://dx.doi.org/10.1128/JVI.01388-13.
13. **Lee PS, Ohshima N, Stanfield RL, Yu W, Iba Y, Okuno Y, Kurosawa Y, Wilson IA.** 2014. Receptor mimicry by antibody F045-092 facilitates universal binding to the H3 subtype of influenza virus. Nat. Commun. **5:**3614. http://dx.doi.org/10.1038/ncomms4614.
14. **Throsby M, van den Brink E, Jongeneelen M, Poon LLM, Alard P, Cornelissen L, Bakker A, Cox F, van Deventer E, Guan Y, Cinatl J, Meulen JT, Lasters I, Carsetti R, Peiris M, de Kruif J, Goudsmit J.** 2008. Heterosubtypic neutralizing monoclonal antibodies cross-protective against H5N1 and H1N1 recovered from human IgM+ memory B cells. PLoS One **3:**e3942. http://dx.doi.org/10.1371/journal.pone.0003942.
15. **Sui J, Hwang WC, Perez S, Wei G, Aird D, Chen L-M, Santelli E, Stec B, Cadwell G, Ali M, Wan H, Murakami A, Yammanuru A, Han T, Cox NJ, Bankston LA, Donis RO, Liddington RC, Marasco WA.** 2009. Structural and functional bases for broad-spectrum neutralization of avian and human influenza A viruses. Nat. Struct. Mol. Biol. **16:**265–273. http://dx.doi.org/10.1038/nsmb.1566.
16. **Okuno Y, Isegawa Y, Sasao F, Ueda S.** 1993. A common neutralizing epitope conserved between the hemagglutinins of influenza A virus H1 and H2 strains. J. Virol. **67:**2552–2558.
17. **Wrammert J, Koutsonanos D, Li G-M, Edupuganti S, Sui J, Morrissey M, McCausland M, Skountzou I, Hornig M, Lipkin WI, Mehta A, Razavi B, Del Rio C, Zheng N-Y, Lee J-H, Huang M, Ali Z, Kaur K, Andrews S, Amara RR, Wang Y, Das SR, O'Donnell CD, Yewdell JW, Subbarao K, Marasco WA, Mulligan MJ, Compans R, Ahmed R, Wilson PC.** 2011. Broadly cross-reactive antibodies dominate the human B cell response against 2009 pandemic H1N1 influenza virus infection. J. Exp. Med. **208:**181–193. http://dx.doi.org/10.1084/jem.20101352.
18. **Ekiert DC, Bhabha G, Elsliger M-A, Friesen RHE, Jongeneelen M, Throsby M, Goudsmit J, Wilson IA.** 2009. Antibody recognition of a highly conserved influenza virus epitope. Science **324:**246–251. http://dx.doi.org/10.1126/science.1171491.
19. **Wyrzucki A, Dreyfus C, Kohler I, Steck M, Wilson IA, Hangartner L.** 2014. Alternative recognition of the conserved stem epitope in influenza A virus hemagglutinin by a VH3-30-encoded heterosubtypic antibody. J. Virol. **88:**7083–7092. http://dx.doi.org/10.1128/JVI.00178-14.
20. **Dreyfus C, Ekiert DC, Wilson IA.** 2013. Structure of a classical broadly neutralizing stem antibody in complex with a pandemic H2 influenza virus hemagglutinin. J. Virol. **87:**7149–7154. http://dx.doi.org/10.1128/JVI.02975-12.
21. **Kashyap AK, Steel J, Oner AF, Dillon MA, Swale RE, Wall KM, Perry KJ, Faynboym A, Ilhan M, Horowitz M.** 2008. Combinatorial antibody libraries from survivors of the Turkish H5N1 avian influenza outbreak reveal virus neutralization strategies. Proc. Natl. Acad. Sci. U. S. A. **105:**5986–5991. http://dx.doi.org/10.1073/pnas.0801367105.
22. **Friesen RHE, Lee PS, Stoop EJM, Hoffman RMB, Ekiert DC, Bhabha G, Yu W, Juraszek J, Koudstaal W, Jongeneelen M, Korse HJWM, Ophorst C, Brinkman-van der Linden EC, Throsby M, Kwakkenbos MJ, Bakker AQ, Beaumont T, Spits H, Kwaks T, Vogels R, Ward AB, Goudsmit J, Wilson IA.** 2014. A common solution to group 2 influenza virus neutralization. Proc. Natl. Acad. Sci. U. S. A. **111:**445–450. http://dx.doi.org/10.1073/pnas.1319058110.
23. **Ekiert DC, Friesen RHE, Bhabha G, Kwaks T, Jongeneelen M, Yu W, Ophorst C, Cox F, Korse HJWM, Brandenburg B, Vogels R, Brakenhoff JPJ, Kompier R, Koldijk MH, Cornelissen LAHM, Poon LLM, Peiris M, Koudstaal W, Wilson IA, Goudsmit J.** 2011. A highly conserved neutralizing epitope on group 2 influenza A viruses. Science **333:**843–850. http://dx.doi.org/10.1126/science.1204839.
24. **Wang TT, Tan GS, Hai R, Pica N, Petersen E, Moran TM, Palese P.** 2010. Broadly protective monoclonal antibodies against H3 influenza viruses following sequential immunization with different hemagglutinins. PLoS Pathog. **6:**e1000796. http://dx.doi.org/10.1371/journal.ppat.1000796.
25. **Corti D, Voss J, Gamblin SJ, Codoni G, Macagno A, Jarrossay D, Vachieri SG, Pinna D, Minola A, Vanzetta F, Silacci C, Fernandez-Rodriguez BM, Agatic G, Bianchi S, Giacchetto-Sasselli I, Calder L, Sallusto F, Collins P, Haire LF, Temperton N, Langedijk JPM, Skehel JJ, Lanzavecchia A.** 2011. A neutralizing antibody selected from plasma cells that binds to group 1 and group 2 influenza A hemagglutinins. Science **333:**850–856. http://dx.doi.org/10.1126/science.1205669.
26. **Dreyfus C, Laursen NS, Kwaks T, Zuijdgeest D, Khayat R, Ekiert DC, Lee JH, Metlagel Z, Bujny MV, Jongeneelen M, van der Vlugt R, Lamrani M, Korse HJWM, Geelen E, Sahin O, Sieuwerts M, Brakenhoff JPJ, Vogels R, Li OTW, Poon LLM, Peiris M, Koudstaal W, Ward AB, Wilson IA, Goudsmit J, Friesen RHE.** 2012. Highly conserved protective epitopes on influenza B viruses. Science **337:**1343–1348. http://dx.doi.org/10.1126/science.1222908.
27. **Tan GS, Krammer F, Eggink D, Kongchanagul A, Moran TM, Palese P.** 2012. A pan-H1 anti-hemagglutinin monoclonal antibody with potent broad-spectrum efficacy in vivo. J. Virol. **86:**6179–6188. http://dx.doi.org/10.1128/JVI.00469-12.
28. **Krammer F, Margine I, Tan GS, Pica N, Krause JC, Palese P.** 2012. A carboxy-terminal trimerization domain stabilizes conformational epitopes on the stalk domain of soluble recombinant hemagglutinin substrates. PLoS One **7:**e43603. http://dx.doi.org/10.1371/journal.pone.0043603.
29. **Margine I, Palese P, Krammer F.** 2013. Expression of functional recombinant hemagglutinin and neuraminidase proteins from the novel H7N9 influenza virus using the baculovirus expression system. J. Vis. Exp. **2013:**e51112. http://dx.doi.org/10.3791/51112.
30. **Carragher B, Kisseberth N, Kriegman D.** 2000. Leginon: an automated system for acquisition of images from vitreous ice specimens. J. Struct. Biol. **132:**33–45. http://dx.doi.org/10.1006/jsbi.2000.4314.
31. **Lander GC, Stagg SM, Voss NR, Cheng A, Fellmann D, Pulokas J, Yoshioka C, Irving C, Mulder A, Lau P-W, Lyumkis D, Potter CS, Carragher B.** 2009. Appion: an integrated, database-driven pipeline to facilitate EM image processing. J. Struct. Biol. **166:**95–102. http://dx.doi.org/10.1016/j.jsb.2009.01.002.
32. **Sorzano COS, Bilbao-Castro JR, Shkolnisky Y, Alcorlo M, Melero R, Caffarena-Fernández G, Li M, Xu G, Marabini R, Carazo JM.** 2010. A clustering approach to multireference alignment of single-particle projections in electron microscopy. J. Struct. Biol. **171:**197–206. http://dx.doi.org/10.1016/j.jsb.2010.03.011.
33. **Yang Z, Fang J, Chittuluru J, Asturias FJ, Penczek PA.** 2012. Iterative stable alignment and clustering of 2D transmission electron microscope images. Structure **20:**237–247. http://dx.doi.org/10.1016/j.str.2011.12.007.
34. **Tang G, Peng L, Baldwin PR, Mann DS, Jiang W, Rees I, Ludtke SJ.** 2007. EMAN2: an extensible image processing suite for electron microscopy. J. Struct. Biol. **157:**38–46. http://dx.doi.org/10.1016/j.jsb.2006.05.009.
35. **Hohn M, Tang G, Goodyear G, Baldwin PR, Huang Z, Penczek PA, Yang C, Glaeser RM, Adams PD, Ludtke SJ.** 2007. SPARX, a new environment for cryo-EM image processing. J. Struct. Biol. **157:**47–55. http://dx.doi.org/10.1016/j.jsb.2006.07.003.
36. **Biasini M, Bienert S, Waterhouse A, Arnold K, Studer G, Schmidt T, Kiefer F, Cassarino TG, Bertoni M, Bordoli L, Schwede T.** 2014. SWISS-MODEL: modeling protein tertiary and quaternary structure using evolutionary information. Nucleic Acids Res. **42:**W252–W258. http://dx.doi.org/10.1093/nar/gku340.
37. **Pettersen EF, Goddard TD, Huang CC, Couch GS, Greenblatt DM, Meng EC, Ferrin TE.** 2004. UCSF Chimera: a visualization system for exploratory research and analysis. J. Comput. Chem. **25:**1605–1612. http://dx.doi.org/10.1002/jcc.20084.
38. **Cohen A, Newland SE, Biddle F.** 1963. Inhibition of influenza virus haemagglutination: a difference of behavior in sera from a single species. Virology **20:**518–529. http://dx.doi.org/10.1016/0042-6822(63)90102-8.
39. **Hai R, Krammer F, Tan GS, Pica N, Eggink D, Maamary J, Margine I, Albrecht RA, Palese P.** 2012. Influenza viruses expressing chimeric hemagglutinins: globular head and stalk domains derived from different subtypes. J. Virol. **86:**5774–5781. http://dx.doi.org/10.1128/JVI.00137-12.
40. **Pica N, Hai R, Krammer F, Wang TT, Maamary J, Eggink D, Tan GS, Krause JC, Moran T, Stein CR, Banach D, Wrammert J, Belshe RB, García-Sastre A, Palese P.** 2012. Hemagglutinin stalk antibodies elicited by the 2009 pandemic influenza virus as a mechanism for the extinction of seasonal H1N1 viruses. Proc. Natl. Acad. Sci. U. S. A. **109:**2573–2578. http://dx.doi.org/10.1073/pnas.1200039109.
41. **Krammer F, Palese P, Steel J.** 10 July 2014. Advances in universal influenza virus vaccine design and antibody mediated therapies based on conserved regions of the hemagglutinin. Curr. Top. Microbiol. Immunol. http://dx.doi.org/10.1007/82_2014_408.
42. **Monto AS, Fleming DM, Henry D, de Groot R, Makela M, Klein T, Elliott M, Keene ON, Man CY.** 1999. Efficacy and safety of the neuramin-

idase inhibitor zanamivirin the treatment of influenza A and B virus infections. J. Infect. Dis. **180:**254–261. http://dx.doi.org/10.1086/314904.
43. **Whitley RJ, Hayden FG, Reisinger KS, Young N, Dutkowski R, Ipe D, Mills RG, Ward P.** 2001. Oral oseltamivir treatment of influenza in children. Pediatr. Infect. Dis. J. **20:**127–133. http://dx.doi.org/10.1097/00006454-200102000-00002.
44. **Harrison SC.** 2008. Viral membrane fusion. Nat. Struct. Mol. Biol. **15:**690–698. http://dx.doi.org/10.1038/nsmb.1456.
45. **Bullough PA, Hughson FM, Skehel JJ, Wiley DC.** 1994. Structure of influenza haemagglutinin at the pH of membrane fusion. Nature **371:**37–43. http://dx.doi.org/10.1038/371037a0.
46. **Chen J, Skehel JJ, Wiley DC.** 1999. N- and C-terminal residues combine in the fusion-pH influenza hemagglutinin HA(2) subunit to form an N cap that terminates the triple-stranded coiled coil. Proc. Natl. Acad. Sci. U. S. A. **96:**8967–8972. http://dx.doi.org/10.1073/pnas.96.16.8967.
47. **Brandenburg B, Koudstaal W, Goudsmit J, Klaren V, Tang C, Bujny MV, Korse HJWM, Kwaks T, Otterstrom JJ, Juraszek J, van Oijen AM, Vogels R, Friesen RHE.** 2013. Mechanisms of hemagglutinin targeted influenza virus neutralization. PLoS One **8:**e80034. http://dx.doi.org/10.1371/journal.pone.0080034.
48. **Jhung MA, Epperson S, Biggerstaff M, Allen D, Balish A, Barnes N, Beaudoin A, Berman L, Bidol S, Blanton L, Blythe D, Brammer L, D'Mello T, Danila R, Davis W, de Fijter S, Diorio M, Durand LO, Emery S, Fowler B, Garten R, Grant Y, Greenbaum A, Gubareva L, Havers F, Haupt T, House J, Ibrahim S, Jiang V, Jain S, Jernigan D, Kazmierczak J, Klimov A, Lindstrom S, Longenberger A, Lucas P, Lynfield R, McMorrow M, Moll M, Morin C, Ostroff S, Page SL, Park SY, Peters S, Quinn C, Reed C, Richards S, Scheftel J, Simwale O, Shu B, Soyemi K, Stauffer J, Steffens C, Su S, Torso L, Uyeki TM, Vetter S, Villanueva J, Wong KK, Shaw M, Bresee JS, Cox N, Finelli L.** 2013. Outbreak of variant influenza A(H3N2) virus in the United States. Clin. Infect. Dis. **57:**1703-1712. http://dx.doi.org/10.1093/cid/cit649.
49. **Chen H, Yuan H, Gao R, Zhang J, Wang D, Xiong Y, Fan G, Yang F, Li X, Zhou J, Zou S, Yang L, Chen T, Dong L, Bo H, Zhao X, Zhang Y, Lan Y, Bai T, Dong J, Li Q, Wang S, Zhang Y, Li H, Gong T, Shi Y, Ni X, Li J, Zhou J, Fan J, Wu J, Zhou X, Hu M, Wan J, Yang W, Li D, Wu G, Feng Z, Gao GF, Wang Y, Jin Q, Liu M, Shu Y.** 2014. Clinical and epidemiological characteristics of a fatal case of avian influenza A H10N8 virus infection: a descriptive study. Lancet **383:**714–721. http://dx.doi.org/10.1016/S0140-6736(14)60111-2.
50. **Anthony SJ, St Leger JA, Pugliares K, Ip HS, Chan JM, Carpenter ZW, Navarrete-Macias I, Sanchez-Leon M, Saliki JT, Pedersen J, Karesh W, Daszak P, Rabadan R, Rowles T, Lipkin WI.** 2012. Emergence of fatal avian influenza in New England harbor seals. mBio **3:**e00166–12. http://dx.doi.org/10.1128/mBio.00166-12.
51. **Collins PJ, Vachieri SG, Haire LF, Ogrodowicz RW, Martin SR, Walker PA, Xiong X, Gamblin SJ, Skehel JJ.** 2014. Recent evolution of equine influenza and the origin of canine influenza. Proc. Natl. Acad. Sci. U. S. A. **111:**11175–11180. http://dx.doi.org/10.1073/pnas.1406606111.